Solvation Dynamics in Dipolar−Quadrupolar Mixtures: A Computer Simulation Study of Dipole Creation in Mixtures of Acetonitrile and Benzene

Branka M. Ladanyi* and Baw-Ching Perng†

Department of Chemistry, Colorado State University, Fort Collins, Colorado 80523

Received: September 20, 2001; In Final Form: May 9, 2002

We present here the results of molecular dynamics simulation of solvation dynamics (SD) in benzene, acetonitrile, and their mixtures corresponding to three sets of acetonitrile mole fractions, $x_{ac} = 0.20$, 0.50, and 0.75, at temperature and densities appropriate for ambient conditions. The change in solute−solvent interactions triggered by solute electronic $S_0 \rightarrow S_1$ excitation is represented as dipole creation in a benzene-like solute. We find that both solvent components are active participants in the SD event, with electrostatic interactions of the dipolar solute with quadrupolar benzene molecules making an important contribution to the solvation mechanism and the steady-state Stokes shift in the fluorescence spectrum. Our model solute is preferentially solvated by acetonitrile in its S_1 state and the enhancement in the local acetonitrile concentration contributes significantly to the solvation time scale, especially in the benzene-rich mixture, where this process becomes considerably slower than the solvation coordinate relaxation in either solvent, in agreement with experimental findings. We investigate the contributions to SD from concentration fluctuations by monitoring the time evolution in the solvation structure. We find that in many respects the way that these fluctuations contribute to SD in benzene−acetonitrile mixtures resembles their contributions to the SD mechanism in mixtures of dipolar molecules.

I. Introduction

Solvent polarity often has strong effects on reaction rates and equilibria in the liquid phase. Polarity can be tuned by mixing a less polar solvent with a more polar one. Even when such mixing leads to a monotonic variation of bulk dielectric properties with composition, the effects on solutes can be more complicated, in view of the fact that preferential solvation by one of the solvent components is likely to occur.[1] Additional complications can arise in solvation dynamics (SD). For typical SD chromophores such as coumarin 153 (C153), the dipole moment changes by about 8 D when the molecule undergoes the $S_0 \rightarrow S_1$ electronic transition.[2] One would expect that the accompanying change in solute−solvent interactions would lead to a change the identity of the mixture component preferentially solvationg the chromophore. Changes in preferential solvation are also likely to strongly affect chemical reactions in which the reactant charge distribution changes as the reaction proceeds. Study of SD in mixtures should therefore provide valuable insights into this molecular aspect of the solvent's influence on chemical reaction dynamics.

The molecular aspects of SD have been an active area of research in recent years and a great deal of progress has been made, as described in several review articles.[3−10] Most of the focus has been on one-component solvents, with a relatively small number of studies devoted to mixtures.[11−23] From this work, information on the contributions of preferential solvation[11−14] and concentration fluctuations[15−21,23] to SD is starting to emerge.

Experiments[16] and molecular dynamics (MD) simulations[21] of SD in methanol−hexane mixtures showed that structural rearrangements associated with a change in preferential solvation do indeed occur and lead to slowing down of the solvent response in hexane-rich mixtures. In the model that was used in the simulation of SD, only the change in the C153−methanol interaction was assumed to contribute to the response, so only the motion of the polar solvent component relative to the solute contributes directly to SD.

A more complex response to an increase in the strength of solute−solvent electrostatic interactions has been found in mixtures in which both components are polar, since they both participate actively in the solvation mechanism.[15,17−20,22−24] Specific cases that have been investigated by MD are same-size Stockmayer molecules with different dipoles,[15,24] water−methanol[19] and water−DMSO mixtures,[19,20] while the experimental studies measured the solvent response to electronic excitation of C153[22,23] and cresyl violet.[25] In all MD studies, the increase in strength in solute−solvent electrostatic interaction has been modeled as a response to charge creation in an atomic solute. Although a number of variations in the response associated with the identities of the solvent components and the sign of the created solute charge were found, there are some common features of the solvation mechanism. Specifically, the short-time response involves solvent reorientation and a compression of the first solvation shell, followed by larger-scale structural rearrangements that lead to enhancement in the concentration of the more polar component in the vicinity of the solute. In mixtures in which the more polar component is dilute, the initial shell compression involves mainly the less polar solvent and leads to a slowing down of SD, since it impedes the local concentration enhancement of the more polar solvent component. This scenario differs from the mechanism of the response of a mixed solvent to a change in the direction of a solute dipole, which had been considered in earlier SD simulations.[13,26]

* Corresponding author. E-mail address: bl@lamar.colostate.edu.
† Present address: Taiwan Semiconductor Manufacturing, 121 Park Ave. III, Science-Based Industrial Park, Hsinchu, Taiwan 300, R.O.C.

10.1021/jp013580a CCC: $22.00
Published on Web 07/10/2002

In the present case, we consider SD in a mixture of acetonitrile and benzene, two solvents, one dipolar and the other quadrupolar, both of which exhibit relatively large static solvatochromic shifts in the fluorescence of chromophores such as C153.[27−29] Given that one can expect benzene to be an active participant in SD, an interesting question is to what extent the solvation mechanism resembles the mechanisms found for dipolar mixtures.

Because benzene lacks a dipole moment, its bulk dielectric properties are not closely related to its solvation properties. Recent MD simulations and integral equation calculations have shown that its finite-wavevector dielectric properties, which are relevant to SD, qualitatively resemble those of polar liquids.[30,31] Benzene and acetonitrile are miscible in all proportions over a wide range of temperatures and pressures, including ambient conditions.[32] The mixture thermodynamic properties deviate relatively weakly from ideal behavior[32] and the dielectric constant increases monotonically as the acetonitrile mole fraction increases.[33] However, as noted above, one might expect that SD will not be as simple. Indeed, recent experiments by the Levinger group[23] indicate that the solvation response slows down at low acetonitrile mole fractions and then speeds up in pure benzene. MD simulation can answer why this occurs by monitoring the separate solvation responses of the two solvent components and by determining the time scale of the appearance of different solvation structural features.

We report here simulation studies of SD in room-temperature benzene−acetonitrile mixtures of varying composition, including pure benzene, in which SD has not yet been investigated by computer simulation. The SD is represented as a dipole creation in a benzene-like solute, with the magnitude of the created dipole resembling that of C153. The roles of the two components and the contributions of preferential solvation changes to the solvent response are investigated. The resulting limitations of the linear response approximation in predicting the solvent response are explored. To make a connection between SD and the properties of benzene−acetonitrile mixtures, we present a brief overview of the variation in the intermolecular structure and single-molecule dynamics as a function of composition. A more complete account of mixture properties will be presented elsewhere.

The remainder of the paper is organized as follows: In section II, we review briefly the theoretical background on SD and define the quantities that we calculate and analyze. The model and computational methods used in our calculations are described in section III. Our results for the structure and dynamics of benzene−acetonitrile mixtures are presented in section IV and for SD in these mixtures in section V. Our main findings are summarized, and the paper is concluded in section VI.

II. Solvation Dynamics—Theoretical Background

Solvation dynamics is typically measured by monitoring the time evolution of the Stokes shift in the fluorescence spectrum of a dissolved chromophore.[6,8] This time evolution is reported usually in terms of the frequency $\nu(t)$ at the peak of the fluorescence band.[6] The experimental solvation response function is given by

$$S_\nu(t) = \frac{\nu(t) - \nu(\infty)}{\nu(0) - \nu(\infty)} \tag{1}$$

where $t = 0$ corresponds to the time of electronic excitation (which occurs essentially instantaneously on the time scale of nuclear motions) and $\nu(\infty)$ corresponds to the peak frequency of the steady-state fluorescence.

Connection to solvation can be made by noting that $\nu(t)$ contains a contribution from the isolated-molecule transition energy (E_{el}) and a time-dependent contribution, $\Delta E(t)$, due to the presence of the solvent[8,34−36]

$$h\nu(t) = E_{el} + \overline{\Delta E(t)} \tag{2}$$

where the overbar indicates an average over all the solute molecules contributing to the observed signal. The solvation response can therefore be expressed as

$$S(t) = \frac{\overline{\Delta E(t)} - \overline{\Delta E(\infty)}}{\overline{\Delta E(0)} - \overline{\Delta E(\infty)}} \tag{3}$$

When $S(t)$ is calculated from computer simulation on a system containing a single solute molecule, the overbar is interpreted as an average over statistically independent nonequilibrium trajectories.

For relatively rigid chromophores typically used to measure SD, the main effect of the change in the electronic state on the solvant environment comes from the change in the solute charge distribution.[28] Other changes, involving solute geometry, polarizability, solute−solvent dispersion and short-range repulsion occur as well but their effects on the time-evolution of the solvatochromic shift and its steady-state value are less pronounced. We will therefore focus here on representing $\Delta E(t)$ as a change in solute−solvent Coulomb interactions due to changes in the solute partial charges. Thus for a system of one solute molecule (molecule 0) and N solvent molecules

$$\Delta E = \sum_{j=1}^{N}\sum_{\alpha\in 0}\sum_{\beta}\frac{\Delta q_{0\alpha} q_{j\beta}}{4\pi\epsilon_0 r_{0\alpha,j\beta}} \tag{4}$$

where $\Delta q_{0\alpha}$ is the change in the partial charge of the solute site α, $q_{j\beta}$ is the partial charge on the site β of the jth solvent molecule and $r_{0\alpha,j\beta}$ is the scalar distance between these two sites. Since the above form of ΔE is pairwise-additive, the contributions to it from different solvent components can be readily identified. In the present case of mixtures of acetonitrile and benzene,

$$\Delta E = \Delta E_{ac} + \Delta E_{be} \tag{5}$$

In a system containing the solute with N_{ac} acetonitrile molecules and $N_{be} = N - N_{be}$ benzene molecules,

$$\Delta E_{ac} = \sum_{j=1}^{N_{ac}}\sum_{\alpha\in 0}\sum_{\beta\in ac}\frac{\Delta q_\alpha q_\beta}{4\pi\epsilon_0 r_{0\alpha,j\beta}} \tag{6}$$

A similar expression, with j ranging from $N_{ac} + 1$ to N and the sum over β running over benzene interaction sites ($\beta \in$ be), applies to ΔE_{be}.

The total solvation response can be readily decomposed into contributions from the two solvent components:

$$S(t) = S_{ac}(t) + S_{be}(t) \tag{7}$$

where for the solvent component A (=ac, be),

$$S_A(t) = \frac{\overline{\Delta E_A(t)} - \overline{\Delta E_A(\infty)}}{\overline{\Delta E(0)} - \overline{\Delta E(\infty)}} \tag{8}$$

If ΔE can be considered to be a small perturbation in system properties, the solvation response can be estimated using the linear response approximation (LRA), which relates $S(t)$ to the time correlation function (TCF) $C_0(t)$ of fluctuations $\delta\Delta E = \Delta E - \langle\Delta E\rangle$ of ΔE in the unperturbed system,[36]

$$C_0(t) = \langle\delta\Delta E(0)\ \delta\Delta E(t)\rangle_0/\langle[\delta\Delta E]^2\rangle_0 \tag{9}$$

where $\langle ...\rangle$ denotes an equilibrium ensemble average for the solvent in the presence of the ground state (S_0) solute.

Previous studies indicate that LRA is not always applicable to solvation dynamics.[13,15,19,20,35,37−41] However, it has proved to be a good approximation for electrostatic SD in acetonitrile,[2,42] one of the solvent components considered here. No evidence is as yet available on its applicability to pure benzene. In some of SD studies in one-component solvents, it has been found that $C_0(t)$ provides a good approximation to $S(t)$ at short times, but that the longer time decay is approximated more accurately by[2,39,43]

$$C_1(t) = \langle\delta\Delta E(0)\ \delta\Delta E(t)\rangle_1/\langle[\delta\Delta E]^2\rangle_1 \tag{10}$$

the TCF of $\delta\Delta E$ for the solvent in the presence of the excited-state (S_1) solute. This reflects the fact that at the longer, diffusive, time scales more information on the change in solute−solvent interaction has been transmitted to the surrounding solvent. Also, the solute motion that is known to contribute substantially to SD at longer times is strongly affected by the change in solute−solvent coupling.

In mixtures, we expect that the LRA will not be able to account for concentration fluctuations associated with changes in preferential solvation. Studies of SD in mixed dipolar solvents have shown that this mechanism leads to a nonlinear response affecting primarily the longer-time portion of $S(t)$.[15,19,20] Deviations of $S(t)$ at longer times from $C_0(t)$ will allow us to gauge the importance of this solvation mechanism in the present system.

Monitoring the changes in the local solvent concentrations more directly by following the time evolution of the solvation structure and coordination numbers in the first solvation shell should shed further light on the SD mechanisms and their time scales. For example, Yoshimori et al.[17,18] and Day and Patey[15] found in the case of ion creation in Stockmayer-molecule mixtures that the populations of the two solvent components in the first solvation shell evolve on two distinct time scales, the shorter one of which they identified with electrostriction and the longer one with redistribution of solvent components. A similar analysis of SD in the present system should reveal to what extent this physical picture applies to mixtures of dipolar and quadrupolar molecules of different sizes and shapes. Specifically, extending their definitions to polyatomic molecules represented by atom−atom potentials, we will monitor the solvent population response in the solvation shells of sites that undergo changes in partial charges by calculating

$$P_{\alpha\beta}(t) = \frac{n_{\alpha\beta}(t) - n_{\alpha\beta}(\infty)}{n_{\alpha\beta}(0) - n_{\alpha\beta}(\infty)} \tag{11}$$

where $n_{\alpha\beta}$ is the first-shell coordination number for solvent atoms of type β in the vicinity of the solute site α.

Even though the LRA is not expected to be valid for long-time SD, we expect that $C_0(t)$ will be a good approximation to $S(t)$ at short times and its further analysis can therefore provide us with insights into other mechanistic aspects of SD in mixed solvents. Given that ΔE is pairwise additive, the decomposition of $C_n(t)$ ($n = 0, 1$) into individual solvent component contributions and their cross correlation can provide us with information on the importance of interspecies cross correlations in SD:

$$\begin{aligned} C_n(t) &= [\langle\delta\Delta E_{ac}(0)\ \delta\Delta E_{ac}(t)\rangle_n + \langle\delta\Delta E_{ac}(0)\ \delta\Delta E_{be}(t)\rangle_n + \\ &\quad \langle[\delta\Delta E_{be}(0)\ \delta\Delta E_{ac}(t)\rangle_n + \langle\delta\Delta E_{be}(0)\ \delta\Delta E_{be}(t)\rangle_n]/\langle(\delta\Delta E)^2\rangle_n \\ &= C_{n,ac}(t) + C_{n,x}(t) + C_{n,be}(t) \end{aligned} \tag{12}$$

Furthermore, assuming that $C_n(t)$ provides a reasonable estimate of the short-time dynamics contributing to $S(t)$, we can learn more about how the velocities of the solute and the two solvent components influence SD by analyzing the "solvation velocity" TCF[44−50]

$$\begin{aligned} G_n(t) &= \langle\Delta\dot{E}(0)\ \Delta\dot{E}(t)\rangle_n \\ &= G_{n,ac}(t) = G_{n,x}(t) + G_{n,be}(t) \end{aligned} \tag{13}$$

where the overhead dot denotes a time derivative and the three contributions are defined as in eq 12.

$\Delta\dot{E}$ can be expressed in terms of solvation forces and torques and molecular center-of-mass and angular velocities:[45]

$$\Delta\dot{E} = -\sum_{j=0}^{N}\sum_{\mu=1}^{6} F_{j\mu}\dot{r}_{j\mu} \tag{14}$$

where $r_{j\mu} = (x_j, y_j, z_j, \theta_j, \phi_j, \psi_j)$ is the coordinate associated with the μth degree of freedom of the jth molecule and $F_{j\mu} = -\partial\Delta E/\partial r_{j\mu}$ is the corresponding force component. We are assuming that the molecules are rigid and that they therefore have only translational (x_j, y_j, z_j) and rotational (θ_j, ϕ_j, ψ_j) degrees of freedom.

Equation 14 can be used to interpret the relative sizes of the three contributions to $G_n(t)$. For example, since the velocities $\dot{r}_{j\mu}$ for different degrees of freedom and different molecules are uncorrelated at $t = 0$, $G_{n,x}(0)$ arises solely from solute motion and can be used to measure how much the solute contributes to the short-time SD. More explicitly, the early decay of $C_n(t)$ can be expressed in terms of the "solvation frequency", $\omega_{n,s}$[45,46,50]

$$C_n(t) = 1 - \frac{\omega_{n,s}{}^2 t^2}{2} + O(t^4) \tag{15}$$

where

$$\omega_{n,s}{}^2 = G_n(0)/\langle(\delta\Delta E)^2\rangle_n \tag{16}$$

Large contributions to $\omega_{n,s}$ will arise from the solvent component for which the mean squared solvation forces or torques and the corresponding mean square velocity components are large, as one can see from eqs 13 and 14

$$G_n(0) = \langle(\Delta\dot{E})^2\rangle_n = \sum_{j=1}^{N}\sum_{\mu=1}^{6}\langle(F_{j\mu})^2\rangle_n\langle\dot{r}_{j\mu}{}^2\rangle_n \tag{17}$$

In the present case, we might anticipate that both force and velocity contributions will favor acetonitrile given that it has a large dipole and that its mass and moments of inertia are smaller than those of benzene.

III. Intermolecular Potentials and Computer Simulation Details

Both solvent components are modeled as rigid, using geometric parameters corresponding to the equilibrium bond

TABLE 1: Intermolecular Potential and Molecular Geometry

A. Acetonitrile[a]

site	(ϵ_α/k_B)/K	σ_α/Å	q_α/e
N	50.24	3.300	−0.514
C	50.24	3.400	0.488
C_m(methyl)	50.24	3.000	−0.577
H	10.04	2.200	0.201

B. Benzene[b]

site	(ϵ_α/k_B)/K	σ_α/Å	q_α/e
C	41.81	3.473	−0.153
H	4.92	2.882	0.153

[a] Bond lengths and angles: $r_{CN} = 1.170$ Å, $r_{CC_m} = 1.460$; $r_{C_mH} = 1.087$; $\angle H-C_m-C = 109.8°$. [b] Bond lengths: $r_{CC} = 1.393$ Å; $r_{CH} = 1.027$ Å.

lengths and angles of isolated molecules. Intermolecular interactions are represented as Lennard-Jones (LJ) + Coulomb atom−atom potentials. For a pair of atoms α and β on different molecules the potential is given by

$$u_{\alpha\beta}(r) = 4\sqrt{\epsilon_\alpha\epsilon_\beta}\left[\left(\frac{\sigma_\alpha+\sigma_\beta}{2r}\right)^{12} - \left(\frac{\sigma_\alpha+\sigma_\beta}{2r}\right)^{6}\right] + \frac{q_\alpha q_\beta}{4\pi\epsilon_0 r} \quad (18)$$

where ϵ_α and σ_α are the LJ potential well depth and diameter and q_α is the partial charge for the atomic interaction site of type α.

In the case of acetonitrile, we use the potential parameters of Böhm et al.[51] and for benzene the parameters correspond to turning the nonelectrostatic, exp-6, portion of the C−C and H−H potentials in the model developed by Williams and coworkers[52,53] into LJ form. The liquid-phase thermodynamic, structural, and transport properties of the resulting model for benzene are essentially identical to those reported by others for the Williams potential.[54−56] The values of parameters specifying the molecular geometries and intermolecular potentials are summarized in Table 1.

Both potentials were chosen because they are relatively simple and because they represent quite well a variety of structural, thermodynamic, and relaxation properties of the pure liquids.[51,54−56] In the case of benzene, for which another LJ + Coulomb site−site potential is also in common use,[57] the Williams potential was chosen because of its properties relevant to electrostatic solvation dynamics: its molecular quadrupole moment is in agreement with experimental data[58] and the liquid-state far-infrared absorption spectrum calculated using this model[56] is in excellent agreement with experiment.[59]

The molecular dynamics (MD) simulations were carried out for pure acetonitrile and benzene and for mixtures corresponding to acetonitrile mole fractions $x_{ac} = 0.20$, 0.50, and 0.75. All systems were at an average temperature of 298 K and at densities corresponding to atmospheric pressure, taken from experimental data of Colin et al.[32] The simulations were carried out on systems of 256 molecules under conditions corresponding to the microcanonical ensemble, using the program MDMPOL,[60a] based on the Verlet leapfrog algorithm for translation,[60] quaternions for rigid-body rotation,[60] and Ewald sums with conducting boundary conditions[60] for the long-range portion of electrostatic interactions. The time steps used in integrating the equations of motion ranged from 4 fs for pure acetonitrile to 8 fs for pure benzene. Equilibrium averages were obtained from trajectories ranging in length from 1.28 to 1.92 ns.

The solvation dynamics event was simulated by designating one of the benzene molecules as the solute and by representing the $S_0 \rightarrow S_1$ electronic transition as an instantaneous change in the partial charges on two of the solute carbons at para positions relative to each other (e.g., carbons 1 and 4) by $+0.5e$ and $-0.5e$. This creates a solute dipole moment of 6.9 D in the solute S_1 state, whereas the S_0 state solute, being benzene-like, has no dipole moment. Even though this solute and the representation of the change in its charge distribution are simpler than for the Coumarin 153 (C153) chromophore used in the experiments, the leading moments in its charge distribution resemble those for C153, which is weakly polar in its ground state and its dipole increases by about 8 D as a result of the $S_0 \rightarrow S_1$ electronic transition.[2]

The results for $S(t)$ and for the related time evolution in the solvation structure were obtained by averaging over 500−600 nonequilibrium trajectories. The starting points, separated by at least 3.2 ps, were chosen from equilibrium benzene−acetonitrile mixture MD data.

IV. Structure and Dynamics of Benzene−Acetonitrile Mixtures

Knowledge about intermolecular structure and dynamics in benzene−acetonitrile mixtures of varying composition can lead to a better understanding of solvation in these systems. We have therefore calculated a number of quantities related to intermolecular structure and translational and rotational dynamics in these systems and present here some of the results. A more complete account of our study of the properties of these mixtures will be given elsewhere.[61]

The systems that we have simulated include a single benzene molecule in acetonitrile (255 molecules), whereas the system containing a single acetonitrile molecule and 255 benzene molecules was not considered. Thus the dilute solution results for only the benzene component are presented.

We present first the results for intermolecular structure in the form of site−site pair correlations, $g_{\alpha\beta}(r)$. Given that acetonitrile has four different types of interaction sites, only a subset of functions involving these sites is shown in Figures 1 and 2, which depict acetonitrile−acetonitrile and acetonitrile−benzene pair correlations. Figure 3 displays all three site pair combinations possible for benzene−benzene $g_{\alpha\beta}(r)$. As all three figures show, both intra- and interspecies pair correlations become more pronounced as the mixtures become richer in benzene. Although the structural enhancement is somewhat larger for the acetonitrile−acetonitrile $g_{\alpha\beta}(r)$'s than for the other component combinations, the fact that it occurs for acetonitrile−benzene pair correlations as well indicates that there is no evidence of strong preference for acetonitrile to surround itself with other acetonitrile molecules. We therefore tentatively explain the sharpening of the intermolecular structure with increasing x_{be} as being due mainly to tighter packing.

Just like the intermolecular structure, the single-molecule dynamics for acetonitrile and benzene change gradually with composition. In Figures 4 and 5 are shown respectively the center-of-mass mean squared displacements, $\langle[\Delta R(t)]^2\rangle$, and the orientational time correlations,

$$\psi_1(t) = \langle \hat{\mathbf{u}}(0)\cdot\hat{\mathbf{u}}(t)\rangle \quad (19)$$

of unit vectors $\hat{\mathbf{u}}$ along molecular axes in mixtures of different x_{ac}. In the case of acetonitrile, this vector is along the molecular dipole (also the 3-fold symmetry axis) and in benzene along a CH bond. The mean squared displacements are related to the

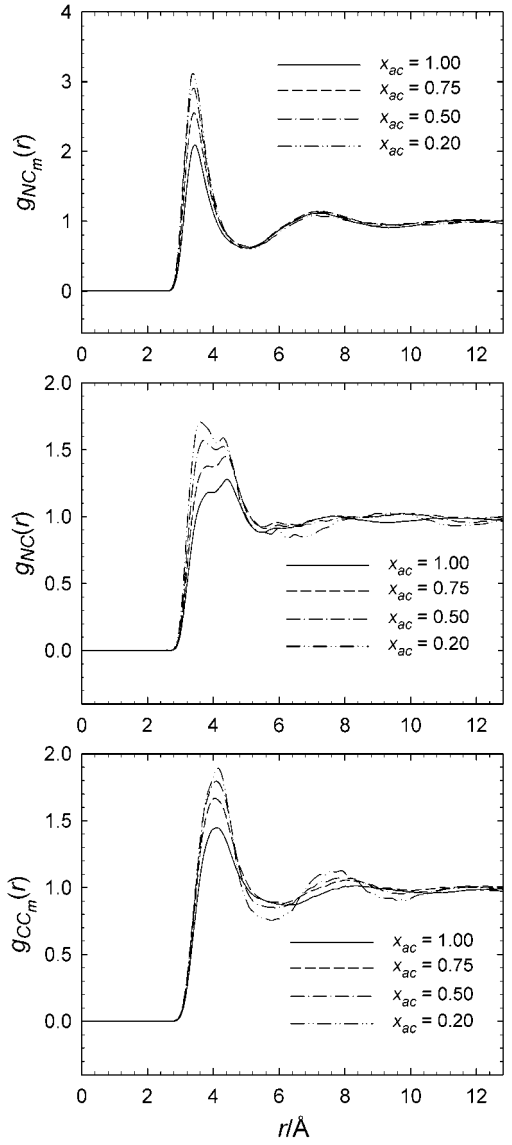

Figure 1. Acetonitrile−acetonitrile atom−atom pair correlations, $g_{NC_m}(r)$ (top panel), $g_{NC}(r)$ (middle panel), and $g_{CC_m}(r)$ (bottom panel), where C_m and C denote, respectively, the methyl and CN group carbons, for pure acetonitrile and in benzene−acetonitrile mixtures corresponding to x_{ac} = 0.75, 0.50, and 0.20.

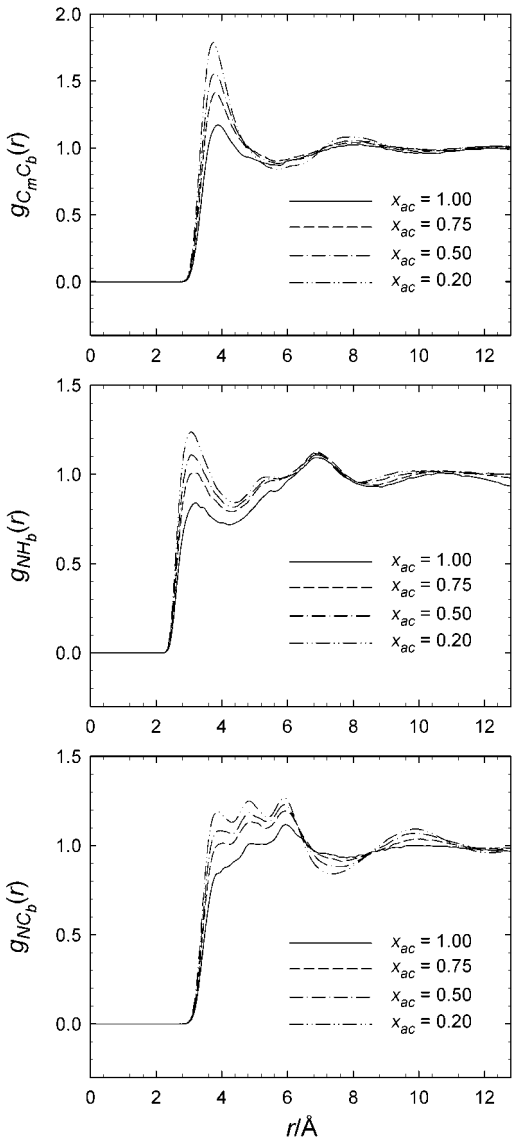

Figure 2. Acetonitrile−benzene atom−atom pair correlations, $g_{C_mC_b}(r)$, $g_{NH_b}(r)$, and $g_{NC_b}(r)$, where the subscript b denotes benzene atoms and C_m is the acetonitrile methyl carbon, for x_{ac} = 255/256, 0.75, 0.50, and 0.20.

molecular self-diffusion coefficients D by

$$6D = \lim_{t\to\infty} \frac{d\langle[\Delta R(t)]^2\rangle}{dt} \tag{20}$$

Table 2 lists the values of D and of the rotational relaxation times

$$\tau_1 = \int_0^\infty dt\, \psi_1(t) \tag{21}$$

for acetonitrile and benzene at several compositions.

Figures 4 and 5 and Table 2 show that both translational diffusion and molecular reorientation slow as the benzene concentration increases. At all concentrations D_{be} is smaller than D_{ac}, as one would expect in view of the larger molecular volume, while the rotational relaxation of the benzene CH vector is faster and less strongly composition-dependent than that of the acetonitrile dipole. Some of the relaxation of the CH vector occurs by the rotation of the molecule about the 6-fold axis,[62,63] displacing very little of the surrounding liquid, so the acetonitrile dipole experiences greater mechanical as well as dielectric friction. For both mixture components, the diffusive portions of $\langle[\Delta R(t)]^2\rangle$ and $\psi_1(t)$ show a monotonic and gradual slowing down with decreasing x_{ac}. This represents further evidence that pronounced structural and dynamical inhomogeneities are absent from these mixtures, at least for the model potentials used here. No structural and dynamical data on acetonitrile−benzene mixtures are available for direct comparison with quantities displayed in Figures 1−5 and Table 2.

V. Solvation Dynamics

A. Solvation Energy Response. Figure 6 depicts the solvation response functions $S(t)$ (eq 3) for pure acetonitrile and benzene and for their mixtures at three compositions. As noted in section II, these are obtained by following the time evolution of the system after one of the benzene molecules instantaneously becomes dipolar through partial charge changes by $e/2$ and $-e/2$ in para-position C-sites.

From the top panel of Figure 6 it can be seen that the short-time portion of $S(t)$ exhibits a smaller initial curvature with increasing x_{be}. This is expected on the basis of the fact that

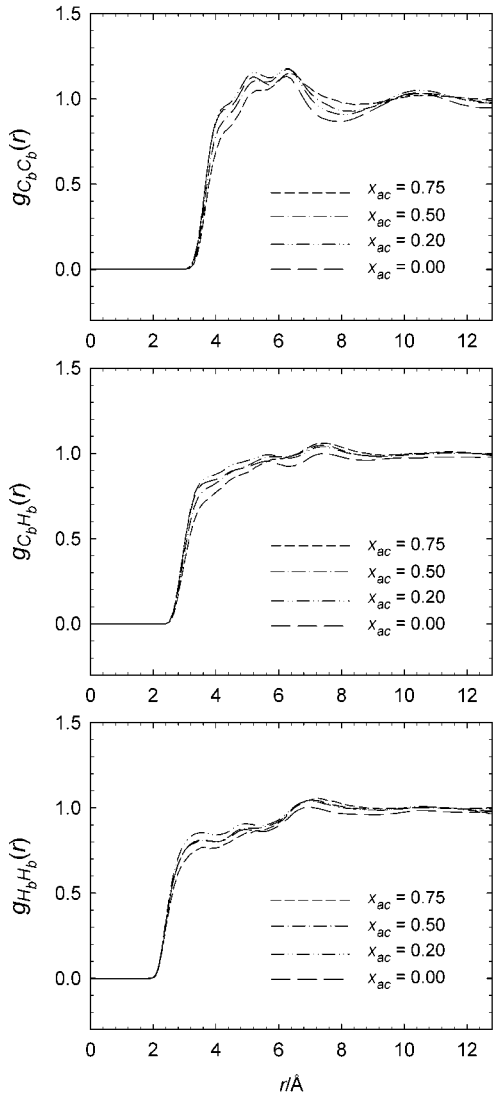

Figure 3. Benzene−benzene atom−atom pair correlations, $g_{C_bC_b}(r)$, $g_{C_bH_b}(r)$, and $g_{H_bH_b}(r)$, where the subscript b denotes benzene atoms, for benzene−acetonitrile mixtures corresponding to $x_{ac} = 0.75$, 0.50, and 0.20 and for pure benzene.

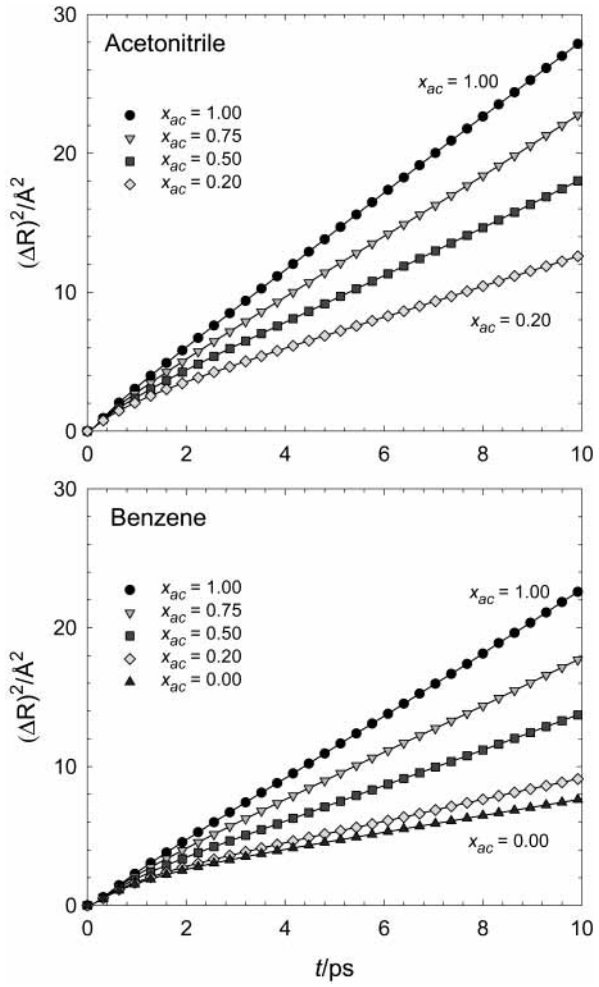

Figure 4. Mean squared displacements of the molecular centers of mass of acetonitrile (top panel) and benzene (bottom panel) molecules. The acetonitrile results are for $x_{ac} = 1.00$, 0.75, 0.50, and 0.20 and the benzene results include also pure benzene ($x_{ac} = 0.00$).

benzene has larger moments of inertia and mass than acetonitrile, both of which will lead to a decrease with increasing x_{be} in the solvation frequency $\omega_{0,s}$ (eq 16). At longer times, slower decay of $S(t)$ with increasing x_{be} occurs in the composition range $0 \leq x_{be} \leq 0.75$. However, in the benzene-rich mixture, $x_{be} = 0.75$, the diffusive decay rate of $S(t)$ becomes slower than in pure benzene, in agreement with experimental results[23,33] indicating that a slowly decaying component becomes increasingly prominent as x_{be} increases in benzene−acetonitrile mixtures, but is absent from $S(t)$ in pure benzene.

Our model chromophore differs from C153 used by Luther et al.,[23] so we do not expect very close agreement with experiment, especially at short times. Experimental $S(t)$ data are usually fit to a sum of exponentials and we have carried out the same fitting procedure for our MD results. The results are given in Table 3. Such a fit is clearly going to be poor at short times, for which $S(t)$ is closer to being Gaussian than exponential, with the initial decay described by eq 15 for $n = 0$. However, the multiexponential form is reasonable at longer times, as the comparison between the MD data and the fit, shown in the bottom panel of Figure 6, illustrates.

In Figure 7 we compare the results of our fit with multiexponential fits to experimental data for the C153 chromophore in acetonitrile,[22] benzene,[23] and their mixtures,[23] at $x_{ac} = 0.50$ and 0.20.

We do not expect perfect agreement between simulation and experiment, especially at short times, given the fact that our model chromophore is smaller and less massive than C153. This will result in a different solvation structure and in a larger contribution of the model solute motion to SD. Nevertheless, we see very good agreement between simulation and experiment at $x_{ac} = 0.5$ and 1.0 over all relevant time scales. In the case of the benzene-rich mixture, $x_{ac} = 0.20$, the agreement is good at long times, but not at shorter times for which the experimental $S(t)$ decays faster, suggesting that there is a higher initial acetonitrile concentration in the first solvation shell of C153 than of the model chromophores in benzene-rich mixtures. The relaxation times τ_3, corresponding to the slowest decay mechanism of $S(t)$ that we obtain from multiexponential fits to our mixed solvent data (Table 3) follow experimental trends and are in quite good agreement with the values obtained from fits to experimental data,[23] which give $\tau_3 = 6.62$ ps at $x_{ac} = 0.5$ and $\tau_3 = 8.73$ ps at $x_{ac} = 0.2$. For solvation in pure benzene our simulation is in only fair agreement with experiment, predicting somewhat faster solvent relaxation than is observed experimentally, despite the fact that some of the pure solvent dynamics, in particular, translational diffusion,[55] are slower in the model system than in the real liquid.

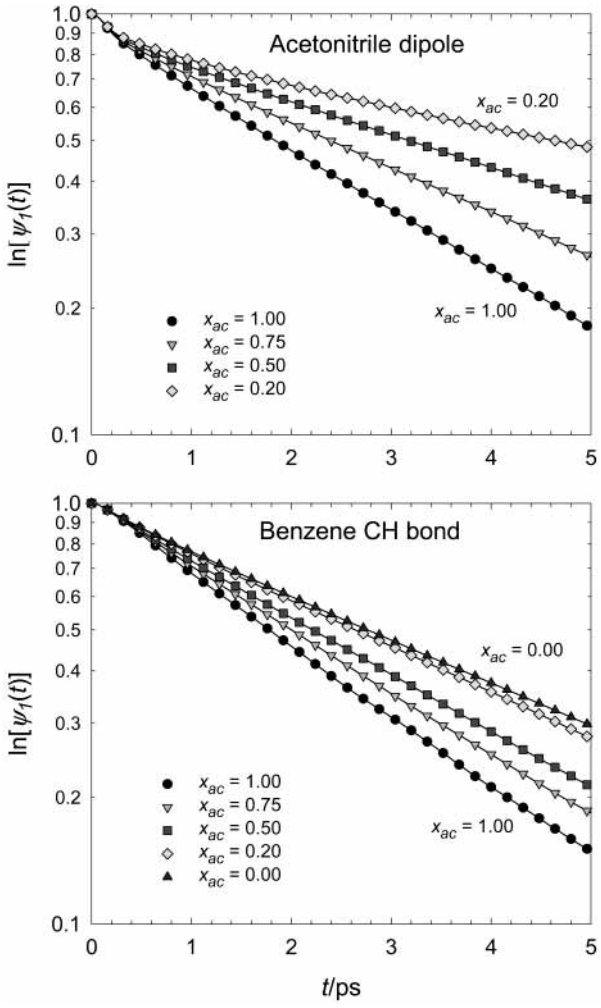

Figure 5. Orientational time correlations, $\psi_1(t)$, of unit vectors along the acetonitrile dipole (top panel) and benzene CH bond (bottom panel) at the same component concentrations as in Figure 4.

TABLE 2: Properties of Benzene−Acetonitrile Mixtures

x_{ac}	v/cm^3 mol^{-1}	$D_{ac}/10^{-9}$ m^2 s^{-1}	$D_{be}/10^{-9}$ m^2 s^{-1}	$\tau_{1,ac}^{CN}$/ps	$\tau_{1,be}^{CH}$/ps
0.00	89.40		1.1		4.1
0.20	81.95	1.9	1.3	7.5	3.9
0.50	71.00	2.8	2.1	4.9	3.3
0.75	61.93	3.6	2.8	3.7	2.9
1.00	52.74	4.6	3.7	2.8	2.7

The experiments and simulation both show that a slowly relaxing component in $S(t)$ is present at $x_{ac} = 0.50$ and 0.20 but absent from the pure solvent components. The presence of this component in the mixtures signals a change in the solvation mechanism. Simulation and theory of solvation dynamics in dipolar mixtures[15,17−19] indicate that the time scale associated with building up enhanced concentration of the more polar solvent component in the vicinity of the solute becomes an important step in the solvation response of mixtures rich in the less polar component. We analyze our MD trajectory data to determine to what extent an analogous mechanism contributes to the present case of dipolar−quadrupolar mixtures.

We start this analysis by presenting in Figure 8 the data for $C_0(t)$ and $C_1(t)$ for the same compositions as the ones depicted in Figure 6. Comparison of Figures 6 and 8 indicates that the short-time dynamics of solvation agrees well with linear response in the presence of the ground-state solute. However, $C_0(t)$ exhibits a slower decay rate with increasing x_{be} at long as well as at short time scales. Thus it does not show a diffusive

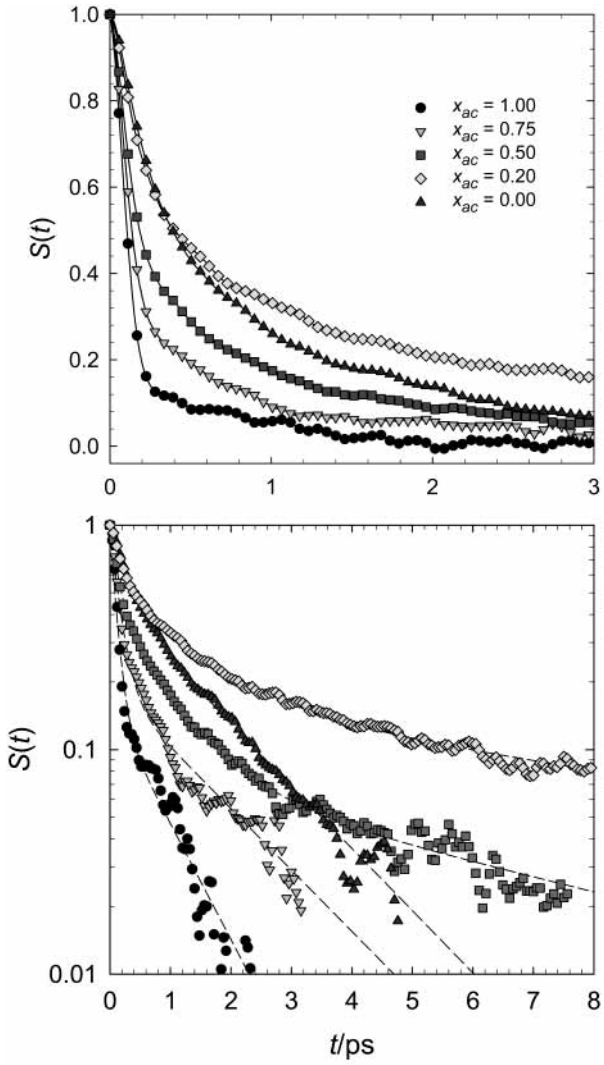

Figure 6. Solvation response function, $S(t)$, following dipole creation in a benzene-like solute in acetonitrile−benzene mixtures at compositions $x_{ac} = 1.00$, 0.75, 0.50, 0.20, and 0.00. The top panel depicts the MD data, focusing on the 0−3 ps time scale. The bottom panel depicts the MD data for ln [$S(t)$] (symbols) and fits of these data to sums of exponentials (dashed lines; see Table 3 for parameters) over a longer time scale.

TABLE 3: Fits of Solvation Response Functions to Sums of Exponentials[a]

x_{ac}	a_1	τ_1/ps	a_2	τ_2/ps	a_3	τ_3/ps
0.00	0.534	0.301	0.466	1.567		
0.20	0.452	0.218	0.379	1.210	0.169	10.8
0.50	0.560	0.138	0.361	0.820	0.079	6.52
0.75	0.808	0.148	0.192	1.588		
1.00	0.846	0.099	0.154	0.842		

[a] The fit is to $S(t) = \sum_i a_i \exp(-t/\tau_i)$ for $t \geq 0.12$ ps. Thus $\sum_i a_i \neq 1$.

decay rate reversal for $x_{be} = 0.80$ and $x_{be} = 1.0$. This further points to a solvation mechanism associated with concentration fluctuations that are absent from the system containing the ground-state solute. The long-time rate reversal for $x_{be} = 0.80$ and $x_{be} = 1.0$ is seen in the case of $C_1(t)$, showing that SD in mixtures becomes nonlinear in benzene-rich mixtures, given that $C_0(t)$ and $C_1(t)$ are in clear disagreement with each other. The differences in the behavior of $C_0(t)$ and $C_1(t)$ may be ascribed to local solvent composition differences in the vicinity of ground- and excited-state solutes, as we shall see below.

To gain further insight into the sources of nonlinearity in solvation in acetonitrile−benzene mixtures, we decompose $S(t)$

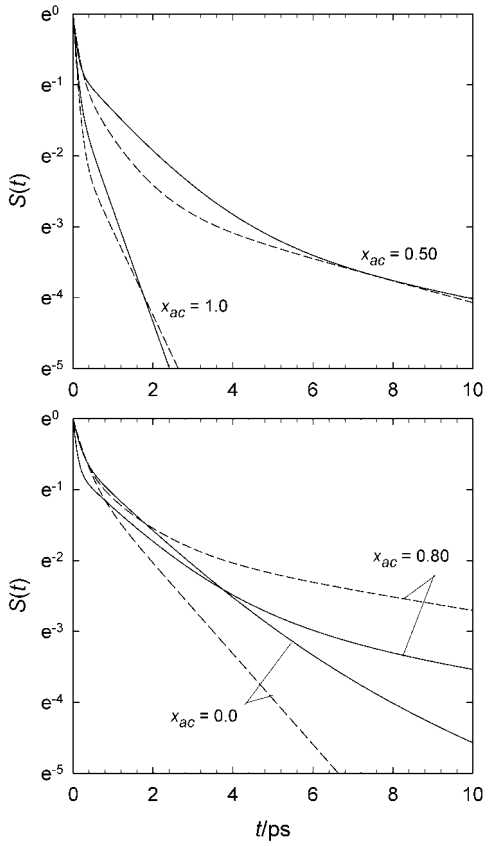

Figure 7. Comparison of the multiexponential fits to the experimental $S(t)$ data for C153 chromophore (full line) and our MD data dipole creation in a benzene-like chromophore (dashed line). The top panel depicts the data for SD in acetonitrile, benzene, and their mixture at $x_{ac} = 0.50$. The bottom panel depicts the data for SD in benzene and in benzene−acetonitrile mixtures at $x_{ac} = 0.20$.

into contributions from the two solvent components and display these results in Figure 9. Given the higher polarity of acetonitrile, $S_{ac}(t)$ dominates the solvent response of the $x_{ac} = 0.75$ and 0.50 mixtures. In the $x_{ac} = 0.20$ mixture, $S_{ac}(t)$ is still larger than $S_{be}(t)$ at short times, but both components play important roles in the overall decay of $S(t)$. In this case it is evident that both $S_{ac}(t)$ and $S_{be}(t)$ exhibit a prominent slowly decaying portion, which is positive for $S_{ac}(t)$ and negative for $S_{be}(t)$. Because of the partial cancellation of the sum of these portions, the amplitude of the slowly decaying part of $S(t)$ is smaller, but still quite prominent. The fact that $S_{be}(t)$ becomes large and negative before decaying to zero suggests that the electrostriction and redistribution solvation steps have opposite effects on the time evolution of ΔE_{be}. This type of behavior of the solvation response of the less polar component has been observed previously in dipolar mixtures at low concentrations of the more highly polar component.[15,19,20] It indicates that benzene is an active participant in SD and that its electrostatic attraction to the excited-state solute plays an important role in the solvation mechanism. It should be noted that the solvent redistribution step is present also at the two higher acetonitrile concentrations, but that its relative importance is smaller in these cases.

Tables 4 and 5 contain information on several aspects of SD. Table 4 contains steady-state Stokes shifts and their contributions from the two solvent components. For the mixtures, these are compared to the results that one would obtain on the basis of ideal mixing. The frequency shift

$$\Delta\nu = [\overline{\Delta E(0)} - \overline{\Delta E(0)}]/hc \qquad (22)$$

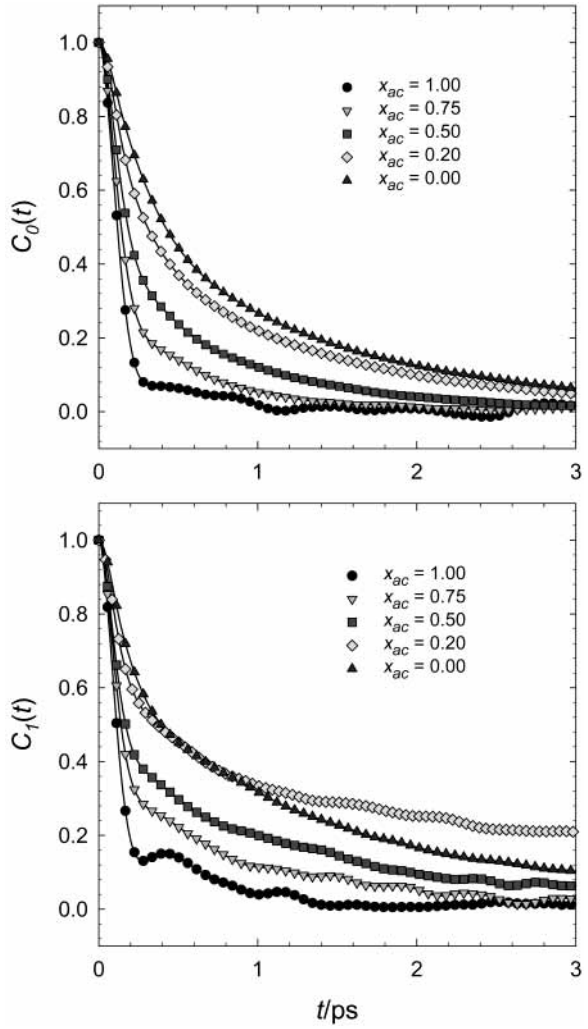

Figure 8. Time correlations, $C_n(t)$, of the fluctuations in the solute−solvent interaction energy change, ΔE, corresponding to solute dipole creation. The top panel depicts $C_0(t)$, the time correlations in the systems containing the ground state, benzene-like, solute and the bottom panel, $C_1(t)$, the time correlation for the systems containing the excited-state dipolar form of the solute. The mixture compositions are as in Figure 6.

is compared to

$$\Delta\nu_{id} = x_{ac}\Delta\nu_{ac,p} + x_{be}\Delta\nu_{be,p} \qquad (23)$$

where the subscript p denotes solution in the pure component.

We see from Table 4 that $\Delta\nu$ in the mixtures is always larger than $\Delta\nu_{id}$ and that this difference can be traced to the fact that acetonitrile contributes more and benzene less to $\Delta\nu$ than one would predict on the basis of ideal mixing. The size of the deviation from ideality increases with increasing benzene concentration, in agreement with experimental trends.[23]

We should note that the values of $\Delta\nu$ that we get for our model solute are of the same order of magnitude measured for the C153 chromophore in the same solvents.[23,29] These are 2.32×10^3 cm^{-1} in pure acetonitrile,[29] in mixtures[23] 1.47×10^3 cm^{-1} at $x_{ac} = 0.50$ and 1.10×10^3 cm^{-1} at $x_{ac} = 0.20$, while two slightly different values,[23,29] 0.72×10^3 and 0.79×10^3 cm^{-1}, have been reported for C153 in pure benzene.

The short-time ($t < 0.2$ ps) dynamics of solvation is represented reasonably well by $C_0(t)$, so we can use the decomposition of $\langle(\delta\Delta E)^2\rangle_0$ and $G_0(0)$ into solvent component contributions to determine how acetonitrile and benzene con-

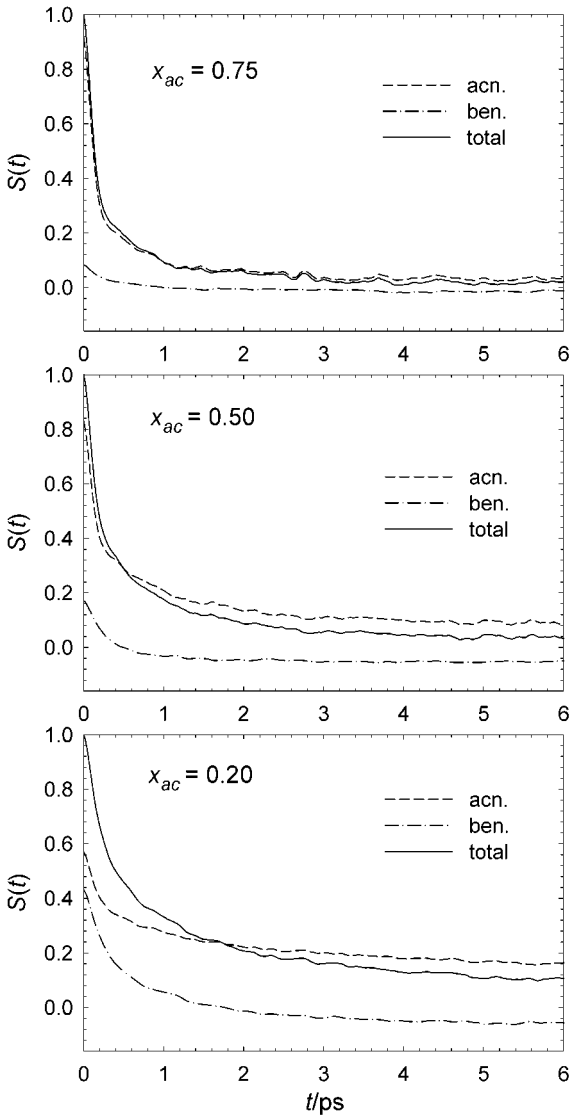

Figure 9. Decomposition of the solvation response function, $S(t)$, into its solvent component contributions, $S_{ac}(t)$ and $S_{be}(t)$, for acetonitrile−benzene mixtures at compositions $x_{ac} = 0.75$ (top panel), $x_{ac} = 0.50$ (middle panel), and $x_{ac} = 0.20$ (bottom panel).

TABLE 4: Steady-State Stokes Shift Values[a]

x_{ac}	$\Delta\nu_{ac}$	$\Delta\nu_{be}$	$\Delta\nu$	$x_{ac}\Delta\nu_{ac,p}$	$x_{be}\Delta\nu_{be,p}$	$\Delta\nu - \Delta\nu_{id}$	$1 - \Delta\nu_{id}/\Delta\nu$
0.00		3.24	3.24		3.24	0.00	0.00
0.20	2.49	1.97	4.46	1.07	2.58	0.80	0.18
0.50	4.08	0.85	4.93	2.69	1.61	0.63	0.13
0.75	4.75	0.43	5.18	4.02	0.81	0.35	0.07
1.00	5.37		5.37	5.37		0.00	0.00

[a] All values are in 1000 cm^{-1}.

tribute to the solvation frequency, $\omega_{0,s}$ (eq 16). These results are given in part A of Table 4. For the sake of completeness, we include in part B of the table the corresponding excited-state data on $\langle(\delta\Delta E)^2\rangle_1$, $G_1(0)$, and $\omega_{1,s}$.

The decomposition of $\langle(\delta\Delta E)^2\rangle_n$ into its species auto and cross correlation contributions indicates that there are strong interspecies cross correlations present in the mixtures. These give rise to negative terms that are similar in magnitude to the benzene autocorrelation contribution at the same composition.

As one might have anticipated on the basis of the smaller mass and moments of inertia of acetonitrile, its contribution to $G_n(0)$ is larger than to $\langle(\delta\Delta E)^2\rangle_n$ (and $C_n(0)$). As a result of this, acetonitrile autocorrelation contribution to $G_n(0)$ exceeds that of $G_{n,be}(0)$ even at $x_{be} = 0.80$. The cross term, $G_{n,x}(0)$, is always small, indicating that solute motion does not play an important role in short-time SD.

Because acetonitrile makes a large relative contribution to $G_n(0)$, there is a large increase in the solvation frequency, $\omega_{n,s}$, in going from pure benzene to the benzene-rich mixture, $x_{be} = 0.80$. $\omega_{n,s}$ increases further as the acetonitrile concentration increases, becoming quite close to the value for pure acetonitrile even at $x_{ac} = 0.50$. The consequences of this are seen in Figures 6 and 8, which show that the short-time decay of $S(t)$ as well as of $C_n(t)$ for $x_{ac} \geq 0.50$ is almost as fast as in pure acetonitrile.

Generally, the differences between the short-time dynamics contributing to $C_0(t)$ and $C_1(t)$ can be attributed to a larger relative contribution of acetonitrile to the solvent response in the S_1 state. These results are consistent with the expected acetonitrile local concentration enhancement in the vicinity of the dipolar form of the solute.

B. Changes in Solvation Structure. Differences in the solvation mechanism between mixtures and one-component solvents are due to concentration fluctuations that can occur only in mixed solvents. They can be observed directly by examining the solvation structure in addition to the time evolution of the solvation energies. In the present case, partial charges on two solute sites are changed to create a dipole in the excited state. We focus on these sites, denoted as + and −, in examining the changes in the solvation structure.

Figures 10 and 11 depict some of the equilibrium solute−solvent pair correlations for the ground (benzene-like) and excited-state solute. Figure 10 depicts the solute−acetonitrile pair correlations $g_{+N}(r)$ and $g_{-C_m}(r)$ at mole fractions $x_{ac} = 0.20$ 0.50, 0.75, and 1.00. While the composition dependence of the ground-state pair correlations is relatively modest, a large increase in the first peak in both pair correlations occurs with decreasing x_{ac}. The bottom panels of the figure show that a local acetonitrile concentration enhancement extending beyond the first solvation shell occurs at $x_{ac} = 0.20$.

In Figure 11 are shown the solute−benzene pair correlations $g_{+C_b}(r)$ and $g_{-H_b}(r)$ at acetonitrile mole fractions, $x_{ac} = 0.00$, 0.20, 0.50, and 0.75. In this case the ground-state pair correlations, which correspond to benzene−benzene functions $g_{C_bC_b}(r)$ and $g_{C_bH_b}(r)$, exhibit relatively weak composition dependence. The excited-state pair correlations for the mixtures show evidence of depletion of benzene from the first solvation shell. Perhaps surprisingly, in view of the Figure 10 results, which show the strongest acetonitrile concentration enhancement at $x_{ac} = 0.20$, the strongest benzene concentration depletion occurs at $x_{ac} = 0.75$ and becomes less pronounced in benzene-richer mixtures.

The results of Figures 10 and 11 are indicative only of the initial and final states and not of the time evolution of the local concentrations. For the three mixture compositions, we have followed the time evolution of the coordination numbers $n_{+\beta}$ and $n_{-\beta}$ for solvent sites β within a shell radius of 5.5 Å from solute sites + and − for all the site pairs depicted in Figures 10 and 11. We found that the time evolution of n_{+N} closely resembles that of n_{-C_m} and that of n_{+C_b} closely resembles n_{-H_b}, so we display the results for only one coordination number per solvent component. These results for the time evolution of n_{+N} and n_{+C_b} over a 10 ps time interval are shown in Figure 12. The figure also shows the equilibrium coordination numbers ($t = \infty$) for the excited-state solute. Several facts about the local compositions can be deduced from the figure. First, it can be seen that as x_{ac} decreases, the relative importance of the solvent redistribution step increases. Second, judging from the distance

TABLE 5: Mixture Component Contributions to Mean Squared Energy Gap Fluctuations and Solvation Velocities

A. Ground State

x_{ac}	$\langle(\delta\Delta E_{ac})^2\rangle_0$/ 10^{-40} J^2	$\langle\delta\Delta E_{ac}\delta\Delta E_{be}\rangle_0$/ 10^{-40} J^2	$\langle(\delta\Delta E_{be})^2\rangle_0$/ 10^{-40} J^2 s^{-2}	$G_{0,ac}(0)$/ 10^{-14} J^2 s^{-2}	$G_{0,x}(0)$/ 10^{-14} J^2 s^{-2}	$G_{0,be}(0)$/ 10^{-14} J^2 s^{-2}	$\omega_{0,s}$/ ps^{-1}
0.00			3.03			0.937	5.56
0.20	2.66	−1.99	2.92	1.09	−0.12	0.80	7.03
0.50	4.22	−2.27	2.10	2.72	−0.13	0.54	8.78
0.75	4.61	−1.49	1.17	4.16	−0.09	0.28	10.1
1.00	4.59			5.66			11.1

B. Excited State

x_{ac}	$\langle(\delta\Delta E_{ac})^2\rangle_1$/ 10^{-40} J^2	$\langle\delta\Delta E_{ac}\delta\Delta E_{be}\rangle_1$/ 10^{-40} J^2	$\langle(\delta\Delta E_{be})^2\rangle_1$/ 10^{-40} J^2 s^{-2}	$G_{1,ac}(0)$/ 10^{-14} J^2 s^{-2}	$G_{1,x}(0)$/ 10^{-14} J^2 s^{-2}	$G_{1,be}(0)$/ 10^{-14} J^2 s^{-2}	$\omega_{1,s}$/ ps^{-1}
0.00			2.18			0.938	6.56
0.20	5.67	−5.60	3.42	1.84	−0.18	0.76	8.31
0.50	5.52	−3.90	2.47	3.87	−0.18	0.49	10.1
0.75	5.85	−3.09	1.68	5.13	−0.13	0.29	10.8
1.00	4.59			6.50			11.9

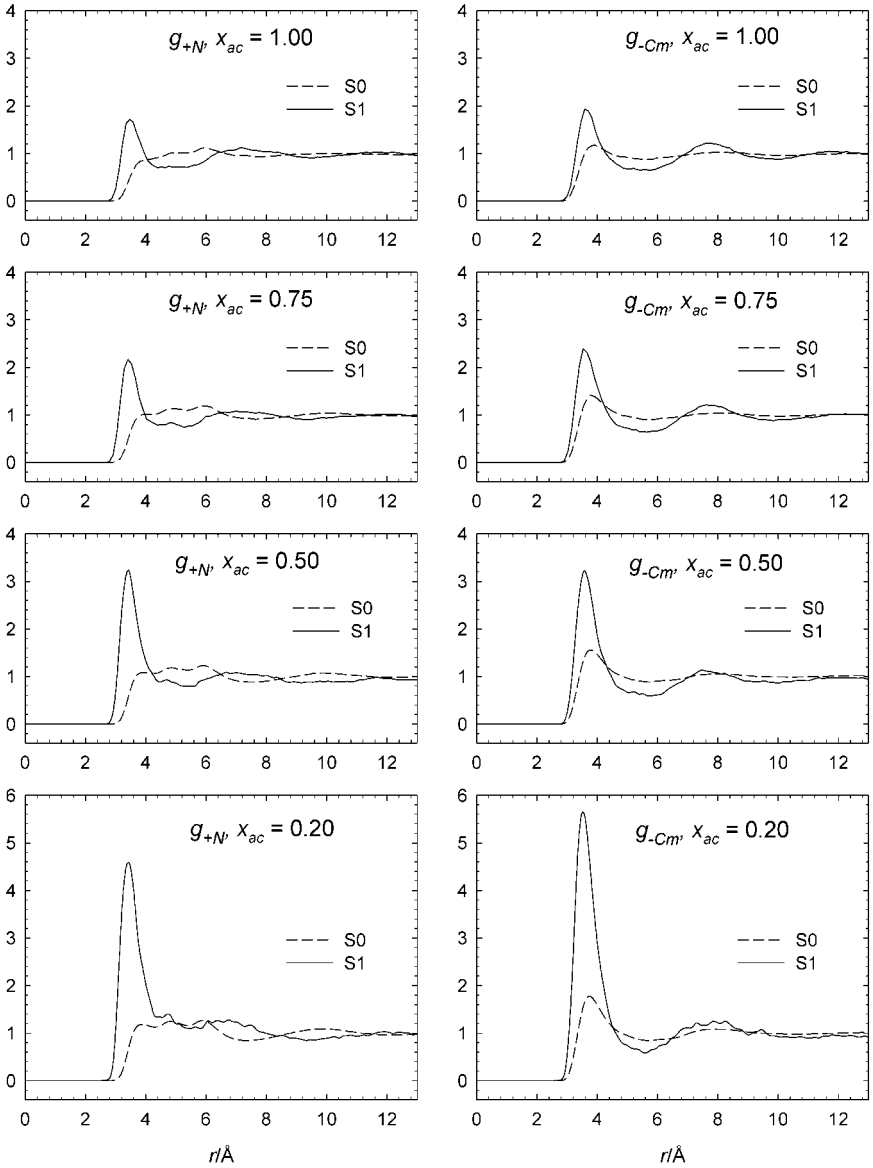

Figure 10. Solute−acetonitrile site−site pair correlations, $g_{+N}(r)$ (left panels) and $g_{-C_m}(r)$ (right panels) for ground (dashed lines) and excited-state (full lines) solutes in acetonitrile−benzene mixtures at x_{ac} = 1.00, 0.75, 0.50, and 0.20 (top to bottom panels).

between coordination numbers at 10 ps and at the S_1 equilibrium, we see that the redistribution step becomes slower at lower x_{ac}. Third, the behavior of the coordination numbers differs qualitatively for the two solvent components. In the case of acetonitrile, n_{+N} increases monotonically to reach the S_1 equilibrium value, while n_{+C_b} first increases and then very gradually decreases, indicating the opposite effects of electrostriction and redistribution in the case of benzene. It should also

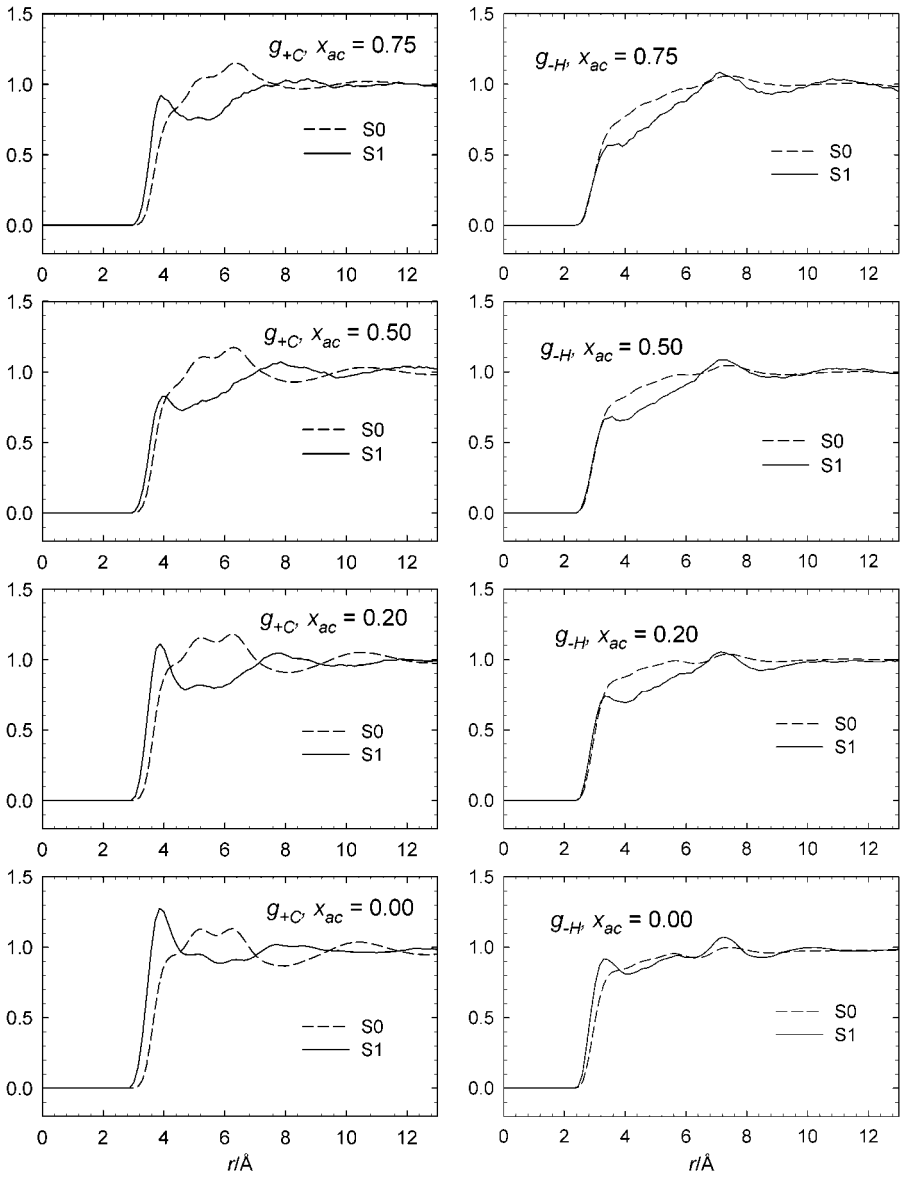

Figure 11. Solute−benzene site−site pair correlations, $g_{+C_b}(r)$ (left panels) and g_{-H_b} (right panels) for ground-state (dashed lines) and excited-state (full lines) solutes in acetonitrile−benzene mixtures at $x_{ac} = 0.75$, 0.50, 0.20, and 0.00 (top to bottom panels).

be noted that the overall change in n_{+C_b} is actually quite small at low benzene concentrations, as exemplified by the $x_{ac} = 0.75$ data. In this case, the relatively modest increase in the local acetonitrile concentration occurs without displacing benzene from the solute vicinity.

The results for the benzene-rich mixture that shows the most pronounced effects of solvent redistribution on SD are further analyzed in Figure 13. The figure depicts the solvent component population relaxation in the form of $P_{+N}(t)$ and $P_{+C_b}(t)$ (see eq 11) in the top panel and the normalized component solvation responses, $S_{ac}(t)/S_{ac}(0)$ and $S_{be}(t)/S_{be}(0)$ in the bottom panel. Both sets of results are over the 0−14 ps time interval, which is considerably longer than the solvation times in the pure components. However, as can be seen from the bottom panel data, neither $S_{ac}(t)$ nor $S_{be}(t)$ are close to having decayed to zero. Their decay rate is rapid within about the first 2 ps, but it then slows down considerably. At times greater than about 2 ps, the solvent redistribution mechanism appears to predominate, as can be seen by comparing SD and solvent population relaxation. The slow monotonic decay of $S_{ac}(t)$ is also seen for $P_{+N}(t)$. In the case of benzene, the fast drop of $S_{be}(t)$ to a minimum value of about −0.2 that occurs on the electrostriction time scale is reflected in the rise in $S_{be}(t)$ to a maximum value of about 2.5. The very slow subsequent increase in $S_{be}(t)$ toward zero tracks the slow decrease in $P_{+C_b}(t)$ after the population maximum has been reached.

The behavior of $S_{ac}(t)$ and $S_{be}(t)$ and of the related component population responses $P_{+N}(t)$ and $P_{+C_b}(t)$ is qualitatively very similar to what Day and Patey[15] found for ion solvation in a binary mixture of Stockmayer molecules at high concentrations of the less polar component, despite the fact that benzene is quadrupolar and not dipolar. This suggests that the basic mechanistic steps of electrostriction and redistribution can be expected to contribute to SD in all mixtures in which electrostatic interactions with both solvent components are significant, even when the leading electric moment is higher than a dipole.

VI. Summary and Conclusion

We have presented here the results of MD simulations of electrostatic solvation dynamics in benzene, acetonitrile and their mixtures corresponding to acetonitrile mole fractions of 0.20, 0.50, and 0.75. Our results were for a benzene-like solute that acquires a dipole, similar in magnitude to the enhancement in

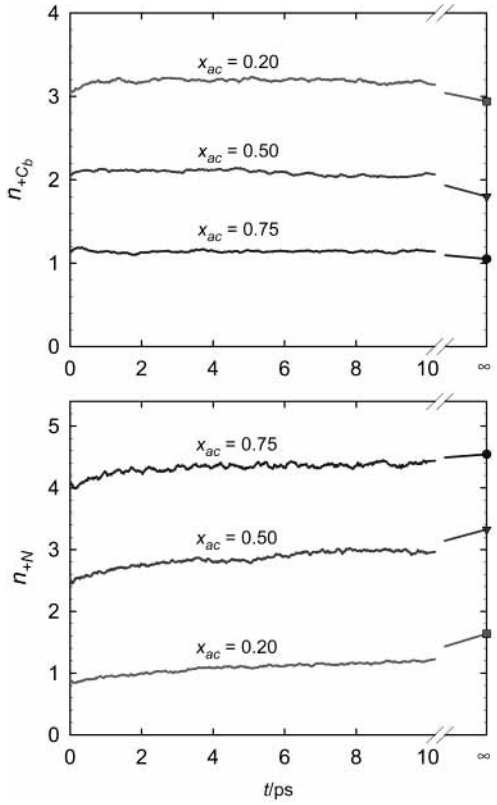

Figure 12. Time evolution of the numbers $n_{+\alpha}(t)$ of solvent atoms in the first solvation shell of the solute site whose charge increases by 0.5*e*. The top panel depicts the solute−benzene solvation numbers n_{+C_b} and the bottom panel the solute−acetonitrile solvation numbers n_{+N}. The three curves in each panel are for mixture compositions $x_{ac} = 0.75$, 0.50, 0.20. The time $t = \infty$ corresponds to the equilibrated excited-state systems.

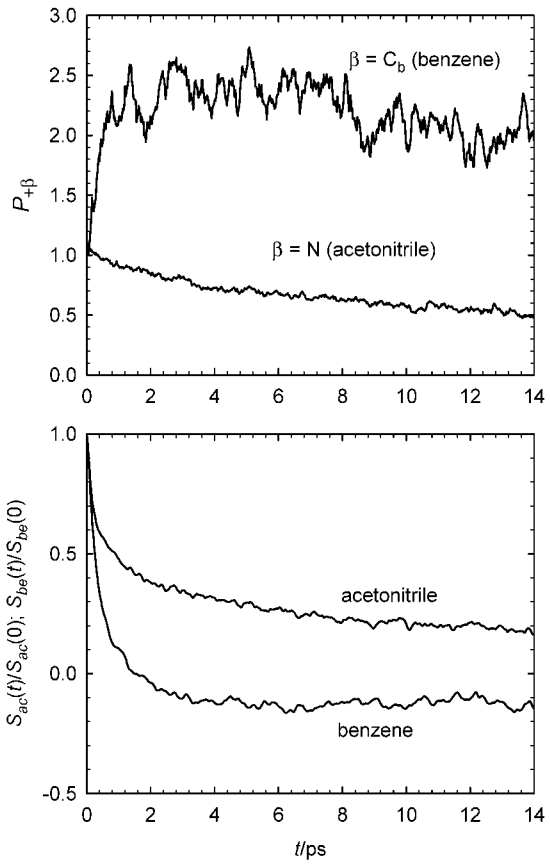

Figure 13. Solvent atom population and solvation energy response in the benzene-rich mixture, $x_{ac} = 0.20$, over the 14 ps time scale. The top panel depicts population relaxation of solvent atoms in the first solvation shell of the solute site whose charge increases by 0.5*e*. Shown are the solute−acetonitrile $P_{+N}(t)$ and solute−benzene $P_{+C_b}(t)$ population responses. The bottom panel depicts the normalized component solvation responses, $S_{ac}(t)/S_{ac}(0)$ and $S_{be}(t)/S_{be}(0)$.

the dipole moment of the C153 chromophore, in its electronically excited state. We have also examined the structure and dynamics of benzene−acetonitrile mixtures to determine to what extent our SD results might be related to preexisting structural inhomogeneities and have investigated the changes in solvation structure that occur upon solute electronic excitation.

We found that no preexisting structural inhomogeneities exist in benzene−acetonitrile mixtures and that rotational and translational relaxation of both solvent components become gradually slower as the benzene concentration increases from $x_{be} = 0.0$ to 1.0. The short-time solvation response follows this trend, but on the diffusive time scale the SD response of the benzene-rich mixture ($x_{be} = 0.80$) becomes considerably slower than for pure benzene, in agreement with the experimentally observed[23,33] behavior of $S(t)$ vs x_{be}. We have shown that the excited-state solute is preferentially solvated by acetonitrile and that the slow solvation time scale is associated with solvent redistribution that produces acetonitrile local concentration enhancement. While solvent redistribution occurs for all the mixture compositions we considered, this mechanistic step makes a significant contribution to the overall SD time scale only in the benzene-rich mixture. In the two mixtures corresponding to lower benzene concentrations, this step makes a significant contribution to the change in the solvation structure, but affects the ΔE to a much smaller extent. This is due in part to the fact that acetonitrile contributes to a greater extent to SD in mixtures than one would predict in terms of ideal solvation and that ΔE can relax to a larger extent through solvent reorientation than is possible for the local solvent population.

The basic steps in SD in the present dipolar−quadrupolar mixtures resemble those seen earlier for ion creation in dipolar mixtures,[15,17−20] without the additional complexities arising from solvent association seen in water−DMSO mixtures.[19,20] These basic steps, termed "electrostriction" and "redistribution" by Day and Patey[15] occur in benzene−acetonitrile mixtures, with benzene assuming the role as the less polar solvent component. In dipolar mixtures, the electrostriction step, which is associated with rearrangements in the nearby solvent molecules, acts to enhance the local concentration of both components in the vicinity of the solute, while the redistribution increases the local concentration of the more polar component at the expense of the less polar one. These mechanistic steps are seen in benzene−acetonitrile mixtures, with the short-time increase, followed by a longer-time decrease in the local benzene concentration especially pronounced and dynamically significant at low acetonitrile concentration. As a result of this, a slow SD step, dominated by translational diffusion, becomes significant in the benzene-rich mixture, as it does for mixtures of dipolar solvents at low concentrations of the more polar component.[15,17−20] An important consequence of this finding is that SD in dipolar−quadrupolar mixtures is not simply related to the SD time scales of the two solvent components but that it can be substantially slower, especially when the time scale associated with solvent redistribution contributes significantly to the overall solvent response. This also strongly suggests that solvent dielectric relaxation is not likely to be closely related to the SD response in dipolar−quadrupolar mixtures. It should be noted that the

SD mechanism in benzene−acetonitrile mixtures differs qualitatively from what has been seen in *n*-hexane−methanol mixtures.[21] The difference comes from the fact that *n*-hexane, which can to a reasonable approximation be considered as apolar, does not actively participate in electrostatic SD. Thus, there is no short-time enhancement in its local concentration in the vicinity of the solute. However, even in that system, the solvent redistribution step leads to a slowing down of SD at low methanol concentrations.[16]

On the basis of our results and those obtained in other simulation studies[15,17,19−21] of electrostatic SD in mixed solvents, one might expect that solvent redistribution will play an important role in the dynamics of charge transfer reactions in mixed solvents, leading to considerably slower reaction rates than those predicted on the basis of the reaction rates in the pure components or on the basis of the rates of molecular relaxation processes in the mixtures in the absence of the reacting solutes. This aspect of reaction dynamics in multicomponent systems definitely deserves further study.

Acknowledgment. Helpful discussions with Professor Nancy E. Levinger and Dr. Bradley M. Luther are gratefully acknowledged. This work was supported by in part by National Science Foundation grants CHE-9520619 and CHE-9981539. Support from the U.S.-Poland Maria Skłodowska-Curie Joint Fund II is also gratefully acknowledged.

References and Notes

(1) Reichardt, C. *Solvents and Solvent Effects in Organic Chemistry*, 2nd ed.; VCH: New York, 1988.
(2) Kumar, P. V.; Maroncelli, M. *J. Chem. Phys.* **1995**, *103*, 3038.
(3) Simon, J. D. *Acc. Chem. Res.* **1988**, *21*, 128.
(4) Bagchi, B. *Annu. Rev. Phys. Chem.* **1989**, *40*, 115.
(5) Maroncelli, M.; MacInnis, J.; Fleming, G. R. *Science* **1989**, *243*, 1674.
(6) Maroncelli, M. *J. Mol. Liq.* **1993**, *57*, 1.
(7) Rossky, P. J.; Simon, J. D. *Nature (London)* **1994**, *370*, 263.
(8) Stratt, R. M.; Maroncelli, M. *J. Phys. Chem.* **1996**, *100*, 12981.
(9) Fleming, G. R.; Cho, M. *Annu. Rev. Phys. Chem.* **1996**, *47*, 109.
(10) Ladanyi, B. M. In *Theoretical Methods in Condensed Phase Chemistry*; Schwartz, S. D., Ed.; Kluwer: Dordrecht, The Netherlands, 2000; p 207.
(11) Chandra, A.; Bagchi, B. *J. Chem. Phys.* **1991**, *94*, 8367.
(12) Chandra, A. *Chem. Phys. Lett.* **1995**, *235*, 133.
(13) Skaf, M. S.; Ladanyi, B. M. *J. Phys. Chem.* **1996**, *100*, 18258.
(14) Skaf, M. S.; Borin, I. A.; Ladanyi, B. M. *Mol. Eng.* **1997**, *7*, 457.
(15) Day, T. J. F.; Patey, G. N. *J. Chem. Phys.* **1997**, *106*, 2782.
(16) Cichos, F.; Willert, A.; Rempel, U.; von Borczyskowski, C. *J. Phys. Chem. A* **1997**, *101*, 8179.
(17) Yoshimori, A.; Day, T. J. F.; Patey, G. N. *J. Chem. Phys.* **1998**, *109*, 3222.
(18) Yoshimori, A.; Day, T. J. F.; Patey, G. N. *J. Chem. Phys.* **1998**, *108*, 6378.
(19) Day, T. J. F.; Patey, G. N. *J. Chem. Phys.* **1999**, *110*, 10937.
(20) Laria, D.; Skaf, M. S. *J. Chem. Phys.* **1999**, *111*, 300.
(21) Cichos, F.; Brown, R.; Rempel, U.; Von Borczyskowski, C. *J. Phys. Chem. A* **1999**, *103*, 2506.
(22) Gardecki, J. A.; Maroncelli, M. *Chem. Phys. Lett.* **1999**, *301*, 571.
(23) Luther, B. M.; Kimmel, J. R.; Levinger, N. E. *J. Chem. Phys.* **2002**, *116*, 3370.
(24) Chandra, A. *Chem. Phys. Lett.* **1995**, *235*, 133.
(25) Nishiyama, K.; Okada, T. *J. Phys. Chem. A* **1998**, *102*, 9729.
(26) Skaf, M. S.; Ladanyi, B. M. *THEOCHEM* **1995**, *335*, 181.
(27) Gardecki, J.; Horng, M. L.; Papazyan, A.; Maroncelli, M. *J. Mol. Liq.* **1995**, *65/66*, 49.
(28) Horng, M. L.; Gardecki, J. A.; Papazyan, A.; Maroncelli, M. *J. Phys. Chem.* **1995**, *99*, 17311.
(29) Reynolds, L.; Gardecki, J. A.; Frankland, S. J. V.; Horng, M. L.; Maroncelli, M. *J. Phys. Chem.* **1996**, *100*, 10337.
(30) Perng, B.-C.; Ladanyi, B. M. *J. Chem. Phys.* **1999**, *110*, 6389.
(31) Ladanyi, B. M.; Perng, B.-C. In *Simulation and Theory of Electrostatic Interactions in Solution*; Pratt, L. R., Hummer, G., Eds.; American Institute of Physics: Melville, NY, 1999; Vol. AIP Conference Proceedings 492; p 250.
(32) Colin, A. C.; Cancho, S.; Rubio, R. G.; Compostizo, A. *J. Phys. Chem.* **1993**, *97*, 10796.
(33) Luther, B. M. Ph.D. Thesis, Colorado State University, 2000.
(34) Bader, J. S.; Chandler, D. *Chem. Phys. Lett.* **1989**, *157*, 501.
(35) Fonseca, T.; Ladanyi, B. M. *J. Phys. Chem.* **1991**, *95*, 2116.
(36) Carter, E. A.; Hynes, J. T. *J. Chem. Phys.* **1991**, *94*, 5961.
(37) Ando, K.; Kato, S. *J. Chem. Phys.* **1991**, *95*, 5966.
(38) Phelps, D. K.; Weaver, M. J.; Ladanyi, B. M. *Chem. Phys.* **1993**, *176*, 575.
(39) Fonseca, T.; Ladanyi, B. M. *J. Mol. Liq.* **1994**, *60*, 1.
(40) Re, M.; Laria, D. *J. Phys. Chem. B* **1997**, *101*, 10494.
(41) Aherne, D.; Tran, V.; Schwartz, B. J. *J. Phys. Chem. B* **2000**, *104*, 5382.
(42) Maroncelli, M. *J. Chem. Phys.* **1991**, *94*, 2084.
(43) Maroncelli, M.; Fleming, G. R. *J. Chem. Phys.* **1988**, *89*, 5044.
(44) Stratt, R. M.; Cho, M. *J. Chem. Phys.* **1994**, *100*, 6700.
(45) Ladanyi, B. M.; Stratt, R. M. *J. Phys. Chem.* **1996**, *100*, 1266.
(46) Ladanyi, B. M.; Stratt, R. M. *J. Phys. Chem.* **1995**, *99*, 2502.
(47) Stratt, R. M. *Acc. Chem. Res.* **1995**, *28*, 201.
(48) Ladanyi, B. M. In *Electron Ion Transfer Condens. Media*; Kornyshev, A. A., Tosi, M., Ulstrup, J., Eds.; World Scientific: Singapore, 1997; p 110.
(49) Ladanyi, B. M.; Stratt, R. M. *J. Phys. Chem. A* **1998**, *102*, 1068.
(50) Ladanyi, B. M.; Maroncelli, M. *J. Chem. Phys.* **1998**, *109*, 3204.
(51) Boehm, H. J.; Lynden-Bell, R. M.; Madden, P. A.; McDonald, I. R. *Mol. Phys.* **1984**, *51*, 761.
(52) Williams, D. E.; Starr, T. L. *Comput. Chem.* **1977**, *1*, 173.
(53) Williams, D. E.; Cox, S. R. *Acta Crystallogr. Sect. B−Struct. Sci.* **1984**, *40*, 404.
(54) Yashonath, S.; Price, S. L.; McDonald, I. R. *Mol. Phys.* **1988**, *64*, 361.
(55) Cabaço, M. I.; Danten, Y.; Besnard, M.; Guissani, Y.; Guillot, B. *J. Phys. Chem. B* **1997**, *101*, 6977.
(56) Danten, Y.; Guillot, B.; Guissani, Y. *J. Chem. Phys.* **1992**, *96*, 3782.
(57) Jorgensen, W. L.; Severance, D. L. *J. Am. Chem. Soc.* **1990**, *112*, 4768.
(58) Battaglia, M. R.; Buckingham, A. D.; Williams, J. H. *Chem. Phys. Lett.* **1981**, *78*, 420.
(59) Besnard, M.; Delcampo, N.; Yarwood, J.; Catlow, B. *J. Mol. Liq.* **1994**, *62*, 33.
(60) (a) Smith, W.; Fincham, D.; *Program MDMPOL*; CCP5 Program Library: Daresbury Laboratory, U.K.; http://www.dl.ac.uk/CCP/CCP5. (b) Allen, M. P.; Tildesley, D. J. *Computer Simulation of Liquids*; Oxford: New York, 1987.
(61) Ladanyi, B. M.; Smith, G. Structure and dynamics of benzene−acetonitrile mixtures. Manuscript in preparation, 2002.
(62) Alms, G. R.; Bauer, D. R.; Brauman, J. I.; Pecora, R. *J. Chem. Phys.* **1973**, *58*, 5570.
(63) Bauer, D. R.; Alms, G. R.; Brauman, J. I.; Pecora, R. *J. Chem. Phys.* **1974**, *61*, 2255.